TECHNICAL NOTE

Analytical Modeling of a Slit Collimator and Optimization for Small Animal Imaging Applications

Etesam Malekzadeh *

Department of Medical Physics, Faculty of Medical Sciences, Tarbiat Modares University, Tehran, Iran

*Corresponding Author: Etesam Malekzadeh
Email: e.malekzadeh1989@gmail.com

Received: 09 September 2022 / Accepted: 09 October 2022

Abstract

Purpose: The collimator design and optimization are essential in small animal molecular imaging for preclinical studies. In this study, a mathematical model was derived and used to optimize the slit collimator for small animal imaging applications.

Materials and Methods: The geometric efficiency was formulated as a source-to-detector distance for a certain amount of the collimator resolution (R_{sys}). The first-order derivative of the derived formula gives the optimized parameters. The detector performance was modeled in terms of intrinsic resolution (R_i). Furthermore, the edge penetration effect was considered using the validated model.

Results: Optimum source-to-detector distance (r_d) was found as $r_d = r_c\left(1.5 + \sqrt{0.25 + 2\left(\frac{R_i}{R_{sys}}\right)^2}\right)$. For an ideal detector, optimal(r_d), geometric efficiency (g_{coll}) and slit aperture width (w) were found as $r_d = 2r_c$, $g_{coll} = \frac{R_{sys}L}{16\pi r_c^2}$ and $w = \frac{R_{sys}}{2}$, respectively. Where r_c and L are the source-to-collimator distance and detector length, respectively. For the fixed resolution of 1.0 mm, the sensitivity for different source-to-collimator distances of 50.0, 100.0, and 150.0 mm was calculated as0.079%, 0.019%, and 0.0088%, respectively. In addition, for a sub-millimeter resolution of 0.5 mm at 15.0, 30.0, and 50.0 mm, the geometric efficiency was calculated as, 0.44%, 0.11%, and 0.039%. For a typical source-to-collimator distance (15.0 mm), the optimal geometric efficiencies are 0.22%, 0.44%, 0.88%, 1.32%, and 1.76% for the resolutions of 0.25, 0.50, 1.0, 1.5, and 2.0 mm, respectively.

Conclusion: Based on the analytic model predictions, the performance characteristics of the slit collimator in terms of geometric efficiency and resolution were extracted. The importance of the proposed model lies both in its speed and ease of application.

Keywords: Mathematical Modelling; Collimator Optimization; Preclinical Imaging; Single Photon Emission Computed Tomography.

DOI: https://doi.org/10.18502/fbt.v11i1.14521

Frontiers in BIOMEDICAL TECHNOLOGIES

1. Introduction

Preclinical animal studies play a key role in drug discovery and development [1]. In these studies, dedicated imaging systems are needed for the anatomical or physiological imaging of small animals [2]. Over the past years, imaging modalities such as Single Photon Emission Computed Tomography (SPECT), Positron Emission Tomography (PET), Computed Tomography (CT), Magnetic Resonance Imaging (MRI), optical imaging, and ultrasonography as an in-vivo, real-time, non-invasive method have been designed and optimized for biodistribution investigations [1,3,4].

Small/medium-animal SPECT is a relatively new imaging instrument that can aid in molecular imaging and drug development science [5]. SPECT is a widely used molecular imaging modality and has the exceptional ability to image many tracers with a broad variety of combinations of isotopes simultaneously [6]. Conventional SPECTs are not suitable for animal imaging because of their low resolution (>1.0 cm), and it is necessary to design high-resolution modalities and dedicated imaging systems [7,8]. The collimator is an important component in SPECT and has a great impact on the overall resolution and efficiency of the system [9]. Therefore, collimator design and optimization are crucial in small animal imaging for preclinical studies.

Much research has been conducted to investigate slit collimators. Gindi *et al.*, in 1992, applied the slit collimators concept for radionuclide tomographic imaging [10]. Their results showed superior performance of slit collimators compared to pinhole collimators. Webb *et al.* derived an analytical formula for collimator efficiency [11]. However, the slit collimator optimization has not been performed based on the derived formula. In Van Holen *et al.*, a study of image quality, achieved with a rotating collimator, was presented [12]. In their study, Monte Carlo simulations were used to study the slit collimator. Mahani *et al.* evaluated the performance of a slit-hole collimator using Monte Carlo simulations for small animal imaging applications [13]. All the mentioned studies use the slit collimator optimized for the special imaging case such as clinical source-to-collimator distance and resolution.

Several collimators have been optimized for small animal imaging applications (Table 1). Collimator design and optimization studies are done using Monte Carlo and analytical modeling [14,15]. MC simulation is time-consuming for finding the suitable set of collimator parameters, which can be used as a roadmap for the design of the study [15]. Also, it is very difficult, if not impossible, to find the theoretical bounds in collimator design using the MC method. On the other hand, analytical modeling is an effective alternative for collimator optimizing and understanding the concepts of the design that overcomes the mentioned problems of the MC method.

Table 1. The geometric efficiencies and resolutions for some of the developed systems

System	Efficiency (%)	Resolution (mm)
FastSPECT-II [16]	0.04	2.5
U-SPECT-I [17]	0.22	0.5
Multi-pinhole SPECT [15]	0.077	0.6
U-SPECT5-E [8]	0.079	2.5
SSR-SPECT [7]	0.007	1.6
SSR [18]	0.016	1.0
SSA-SPECT-1 [14]	0.09	1.1

The idea of modeling a slit collimator was motivated by the recent applications of multi-pinhole collimators in the field of animal imaging [19,20]. The main advantage of a slit collimator compared to the pinhole collimator is its long and narrow slit pattern instead of the conventional square shape of a pinhole [21]. Therefore, the slit pattern could collect more photons than the square or circle-shaped collimators. Also, slit collimators can offer a superior spatial resolution than square-shaped pinhole collimators, given the equivalent detector areas [21].

To the best of our knowledge, no analytical model has been developed for the slit collimator design and optimization. Therefore, this study aims (i) to derive an analytical model of the slit collimator (ii) to apply the model for studying the slit collimator characteristics in terms of geometric efficiency and resolution and (iii) to exploit the model for design optimization of the slit collimator.

2. Materials and Methods

A mathematical model was derived and used to optimize the slit collimator. Our optimization procedure is a new adaption from the method described by Rentmeester *et al.* [15] to determine the imaging system parameters that provide the best performance. The method is based on the geometric trade-off between system resolution and geometric efficiency. Therefore, according to this method, a relationship must be obtained between the resolution and the efficiency of the collimator. To do so, the geometric efficiency of the collimator was formulated in terms of the source-to-detector distance for a certain amount of the collimator resolution. Then, by setting the first derivative of the obtained equation to zero, the optimized parameters were calculated. The detection efficiency was calculated in the middle of the defined FOV. The conceptual diagram of the collimator and its geometric parameters are illustrated in Figure 1.

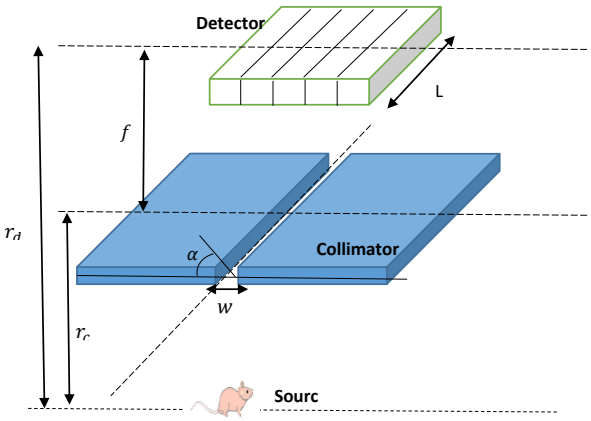

Figure 1. The conceptual diagram of the slit camera geometry is shown. The parameters are slit aperture width, w, source-to-collimator distance, r_c, source-to-detector distance, r_d, focal length, f, and detector length, L. The typical source-to-collimator distances for the preclinical small animal imaging and clinical brain imaging are 15.0 and 150.0 mm, respectively [1, 2, 7, 22, 23]

An adaptation of Metzler's method [24] was used to provide a way of calculating the resolution of the camera, R_{sys}. According to this method, it was assumed that the total resolution of the slit collimator can be calculated by combining the slit collimator resolution R_{slit} and intrinsic resolution R_i of the pixelated detector that is given by the following Equation:

$$R_{sys} = \left[R_{slit}^2 + \left(\frac{r_c}{r_d - r_c}\right)^2 R_i^2\right]^{\frac{1}{2}} \quad (1)$$

In Equation 1, R_{slit} is the slit collimator geometrical resolution given with the following Equation:

$$R_{slit} = w\frac{r_d}{r_d - r_c} \quad (2)$$

The collimator efficiency (g_{coll}) of the KE slit camera can be as follows [25]:

$$g_{coll} = \frac{wL}{4\pi r_d r_c} \quad (3)$$

With combining Equation 1 and Equation 3, the collimator efficiency g_{coll} was calculated as follows. As such, the model of a slit collimator is (Equation 4):

$$g_{coll} = \left[R_{sys}^2 - \left(\frac{r_c}{r_d - r_c}\right)^2 R_i^2\right]^{\frac{1}{2}} \frac{L(r_d - r_c)}{4\pi r_d^2 r_c} \quad (4)$$

With $x = \frac{r_d - r_c}{r_c}$ then $r_d = r_c(1 + x)$, Equation 4 reads (Equation 5):

$$g_{coll} = \left[R_{sys}^2 - \left(\frac{R_i}{x}\right)^2\right]^{\frac{1}{2}} \frac{L\,x}{4\pi r_c^2 (1 + x)^2} \quad (5)$$

With $\frac{d}{dx} g_{coll} = 0$ and some mathematical work results in (Equation 6):

$$R_{sys}^2 x^2 - R_{sys}^2 x - 2R_i^2 = 0 \quad (6)$$

Solving this equation for x gives (Equation 7):

$$x = 0.5 \pm \sqrt{0.25 + 2\left(\frac{R_i}{R_{sys}}\right)^2} \quad (7)$$

Note that $x = 0.5 - \sqrt{0.25 + 2\left(\frac{R_i}{R_{sys}}\right)^2}$ is always zero or negative. In this situation, $r_d = r_c$, which is an unrealistic condition where the detector is in the collimator position. It is obvious that our developed model can't interpret such an unrealistic case. Finally, the optimum source-to-detector distance is (Equation 8):

$$r_d = r_c\left(1.5 + \sqrt{0.25 + 2\left(\frac{R_i}{R_{sys}}\right)^2}\right) \quad (8)$$

For an ideal detector (i.e., $R_i = 0$) the model predicts $r_d = 2r_c$, which gives the maximum efficiency as (Equation 9):

$$g_{coll} = \frac{R_{sys}L}{16\pi r_c^2} \quad (9)$$

And optimal slit aperture width is (Equation 10):

$$w = \frac{R_{sys}}{2} \quad (10)$$

The edge penetration was not taken into account in the optimization step, but the efficiency calculations include the penetration through the collimator slit edge.

For a slit collimator, the edge penetration was taken into account with a validated model [26] as (Equation 11):

$$w_{eff} = w + \frac{1.0}{\mu \times tan(\alpha)} \quad (11)$$

For ^{99m}Tc radiopharmaceuticals, the linear attenuation coefficient for tungsten is $\mu = 3.6\ mm^{-1}\ at\ 140.0\ keV$ [27].The opening angle, α, is always chosen as small as possible to maximize the stopping power of the slit aperture material without truncating the projected FOV on the detector. In this study, we defined the slit angle for the slit collimator (Figure 1). The relation between the slit angle and the opening angle is $\alpha + \frac{\beta}{2} = \frac{\pi}{2}$, where α and β are the slit angle and opening angle, respectively. Therefore, the slit angle was calculated using the opening angle formula as $\frac{\pi}{2} - arcsin(FOV/2r_c)$ [15].

3. Results

The optimum source-to-detector distance (r_d) was found as $r_d = r_c\left(1.5 + \sqrt{0.25 + 2\left(\frac{R_i}{R_{sys}}\right)^2}\right)$. For an ideal detector, optimal (r_d), geometric efficiency (g_{coll}), and slit aperture width (w) were found as $r_d = 2r_c$, $g_{coll} = \frac{R_{sys}L}{16\pi r_c^2}$and $w = \frac{R_{sys}}{2}$, respectively.

Based on the derived formulas, the results are reported in Table 2. For the fixed resolution of 1.0 mm, the sensitivity for different source-to-collimator distances of 50.0, 100.0, and 150.0 mm was calculated as0.079%, 0.019%, and0.0088%, respectively. In addition, for a sub-millimeter resolution of 0.5 mm at 15.0, 30.0, and 50.0 mm, the geometric efficiency was calculated as, 0.44%, 0.11%, and 0.039%.

For small animal studies such as mice, the smaller rings (i.e., source-to-collimator distances) are required. In Figure 2, for a typical source-to-collimator distance (15.0 mm) and an ideal detector, the optimal geometric efficiencies are 0.22%, 0.44%, 0.88%, 1.32%, and 1.76% for the resolutions of 0.25, 0.50, 1.0, 1.5, and 2.0 mm, respectively. The geometric efficiency versus resolution was plotted in Figure 2 for other possible source-to-collimator distances.

Apart from small animal imaging, some collimators are designed for medium size animal imaging like rabbits. Optimal collimator designs were investigated using the developed model and reported.

Table 2. The slit collimator optimization results were reported for different supposed configurations of the small/medium size animal imaging

Source to collimator distance (mm)	Source to detector distance (mm)	Focal length (mm)	Resolution (mm)	Slit width(mm)	Efficiency (%)
15	30	15	0.5	0.25	0.44
30	60	30	0.5	0.25	0.11
50	100	50	0.5	0.25	0.039
50	100	50	1	0.5	0.079
100	200	100	1	0.5	0.019
150	300	150	1	0.5	0.0088

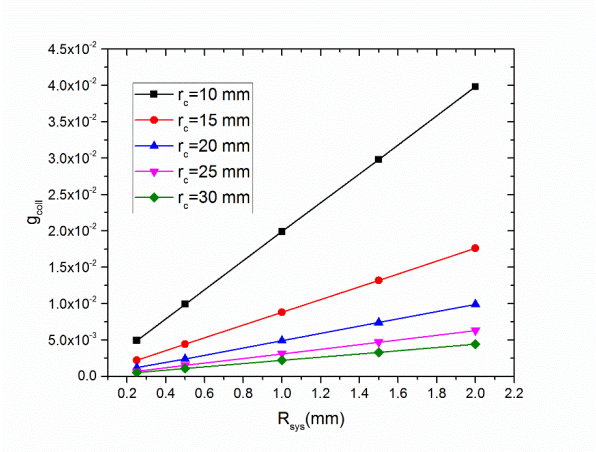

Figure 2. The optimal geometric efficiencies of the slit collimator are plotted versus geometric resolution for different source-to-collimator distances. The detector was supposed ideal

In Figure 3, the optimized geometric efficiency of the slit collimator against the resolution is reported for typical source-to-collimator distances of 30.0 and 100.0 mm. For the systems in Table 1, the efficiency of the detector is also included in the sensitivity calculation by the researchers.

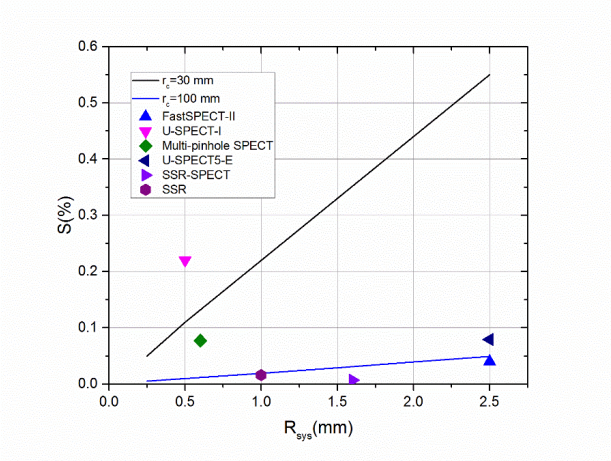

Figure 3. The amounts of the geometric efficiencies (i.e., sensitivity) against the resolution are plotted for the slit collimator and six different imaging systems. For the slit collimator, the detector was supposed ideal

The optimal ratio was calculated versus intrinsic resolution for the different system resolutions. In Figure 4, a ratio of 2.0 is obtained for high-resolution detectors that is approximately independent of the system resolution.

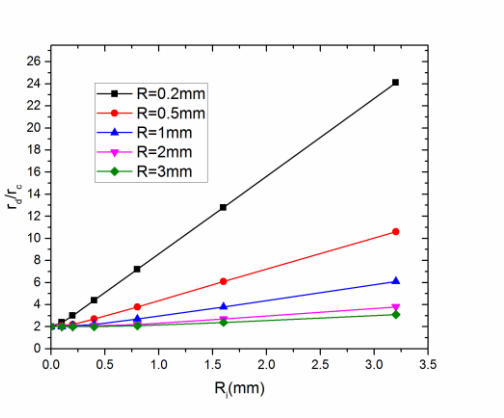

Figure 4. Detector distance to slit distance ratio against the intrinsic resolution for different system resolutions is shown

For small animal imaging with a given condition (FOV=20.0 mm, slit distance=15.0 mm), the slit angle of 50 degrees was calculated. Putting these values in Equation 11, a 0.23 mm additional aperture width was obtained that is considerable in small animal imaging device optimization. In Table 3, the optimal sensitivity amounts are reported for slit cameras with Conventional Detector Systems (CDS) and High-Resolution Detector Systems (HRDS). The CDS was assumed an NaI(Tl) crystal with a 3.2 mm intrinsic resolution [15]. The HRDS detector was considered HICAM prototype with less than 1.0 mm resolution [22].

The edge penetration has a small contribution (less than 14%) to the sensitivity for low-resolution system (Table 3). On the other hand, for high-resolution designs, edge penetration significantly affects the sensitivity (up to 70%). In addition, the penetration through the collimator slit has a small contribution to the sensitivity for large slit angles (Table 4). Further studies may consider the penetration for high-energy emitting radioisotopes.

4. Discussion

In this study, we derived an analytical model for slit collimator design and optimization purposes. Using the developed model, the optimization of the slit collimator for small/medium size animal imaging was studied completely. It was found that for a given resolution and source-to-collimator distance, there is a unique configuration of the collimator parameters that lead to maximum geometric efficiency. Moreover, it

Table 3. Sensitivities of the optimized slit collimator for a small animal imaging system with conventional detector system (CDS) and high-resolution detector system (HRDS). The intrinsic resolution of CDS and HRDS detectors are 0.1 and 3.2 mm, respectively. Source-to-collimator distance fixed at 15.0 mm. L=100.0 mm

	Sensitivity (%)			
	CDS (3.2 mm)		HRDS (0.1 mm)	
Fixed Resolution(mm)	Without penetration	With penetration	Without penetration	With penetration
0.2	0.02	0.05(+60%)	0.14	0.47(+70%)
0.5	0.10	0.17(+41%)	0.36	0.76(+53%)
1	0.34	0.46(+26%)	0.78	1.17(+33%)
2	1.00	1.20(+17%)	1.57	1.96(+20%)
3	1.78	2.03(+12%)	2.36	2.75(+14%)

Table 4. Sensitivities are reported for the camera with HRDS detector (intrinsic resolution is 0.1 mm) with considering the edge penetration and without it. The ratio is calculated as sensitivity with edge penetration to sensitivity without edge penetration. Source-to-collimator and system resolution was fixed at 15.0 and 1.0mm, respectively. FOV is 20.0 mm

	Sensitivity (%)		
Slit angle (degree)	Without penetration	With penetration	Ratio
30	0.76	1.49	1.9
45	0.76	1.18	1.5
60	0.76	1.01	1.3
90	0.76	0.76	1.0

was found the optimal configuration is only dependent on the source-to-collimator distance, system resolution, and intrinsic resolution. Furthermore, the results show the magnification effect vanishes if using high-resolution detectors (Figure 4). Consequently, compact cameras could be fabricated with high-resolution detectors. On the other hand, using conventional NaI crystals with 3.2 mm resolution, the magnification effect is necessary to achieve high overall resolution.

The study showed that the geometric efficiency is linearly related to the resolution (Figure 2). This interesting finding is in agreement with the results obtained by Lopez *et al.* and Zeng *et al.* for the slit collimator [21,28]. However, it contradicts the results reported in the literature for physical collimators of parallel holes and pinholes that the geometric efficiency is proportional to the square of the resolution [9].

The performance characteristics in terms of geometric efficiency and resolution are comparable to developed systems in the literature. However, the detector was supposed ideal in this study. The detector response may be taken into account by multiplying geometric efficiencies and intrinsic efficiency. The NaI(Tl) crystal has an intrinsic efficiency of 0.89 [15]. Then, the modified optimal geometric efficiencies at 30.0 and 100.0 mm are 0.097% and 0.043% for which the resolution is 0.5 and 2.5 mm, respectively. The resolution and sensitivity of the Multi-pinhole SPECT system at 24.0 mm are 0.6 mm and 0.077%, respectively (Table 1).

The Monte Carlo method is used for some aspects of gamma camera simulation, such as scattering consideration, which can hardly be modeled with the analytical methods [9, 29]. However, MC is time-consuming and it is difficult to check all the conditions of the interdependent variables for geometrical optimization of an imaging system, such as Slit-Slat or knife-edge-shaped slit cameras [22]. As an alternative, an analytical method is a fast, reliable, and effective calculation technique to evaluate the geometric parameters of an imaging camera that is widely used for imaging modality design optimization.

The main aim of this study was to develop an analytical model for slit collimator design and optimization. For further studies, the effect of the penetrated and scattered photons from the collimator could be considered to complete the developed model in this study. Also, the detector response in terms of intrinsic resolution and efficiency could be studied using another numerical computational method such as MC simulation which is beyond the scope of this research.

5. Conclusion

Analytical models are powerful tools for slit collimator design and optimization. The performance characteristics of the slit collimator in terms of geometric efficiency and resolution are comparable to the reported results in the literature. Therefore, the derived model could be generalized to other types of collimators. The importance of the proposed model lies both in its speed and relative straightforwardness of application.

Appendix

Starting with Equation 5, we provide the readers with the derivation of Equation 6 here.

$$g_{coll} = \left[R_{sys}^2 - \left(\frac{R_i}{x}\right)^2\right]^{\frac{1}{2}} \frac{L\,x}{4\pi r_c^2 (1+x)^2} \qquad (5)$$

Rewriting Equation 5 and omitting the coefficient $\frac{L}{4\pi r_c^2}$ gives:

$$g_{coll} = \left[R_{sys}^2 x^2 - R_i{}^2\right]^{\frac{1}{2}} \frac{1}{(1+x)^2}$$

Taking the first derivation gives

$$\frac{1}{2}\left(2R_{sys}^2 x\right)\left(R_{sys}^2 x^2 - R_i^2\right)^{-1/2}(1+x)^2 - 2(1+x)\left(R_{sys}^2 x^2 - R_i^2\right)^{\frac{1}{2}} = 0$$

With some algebraic calculations

$$\left(R_{sys}^2 x\right)(1+x)^2 - 2(1+x)\left(R_{sys}^2 x^2 - R_i^2\right) = 0$$

Then:

$$(1+x)\left[\left(R_{sys}^2 x\right)(1+x) - 2\left(R_{sys}^2 x^2 - R_i^2\right)\right] = 0$$

One possible answer comes from $1+x=0$ solution, which is unlikely, because it results in $r_d = 0$.

Continuing with $\left(R_{sys}^2 x\right)(1+x) - 2\left(R_{sys}^2 x^2 - R_i^2\right)=0$ gives:

$$R_{sys}^2 x + R_{sys}^2 x^2 - 2R_{sys}^2 x^2 + 2R_i^2 = 0$$

Finally, some algebraic simplifications result in Equation 6:

$$R_{sys}^2 x^2 - R_{sys}^2 x - 2R_i^2 = 0 \qquad (6)$$

In Figure 5, Equation 5 was plotted as a function of x for the HRDS (0.1 mm) detectors where the system resolution and source-to-collimator distance are supposed fixed at 1 mm and 15 mm, respectively. FOV is 20.0 mm.

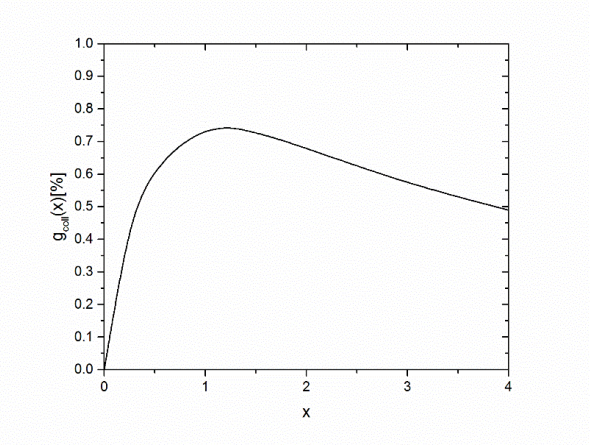

Figure 5. The collimator efficiency is plotted as a function of x, which is defined as $\frac{f}{r_c}$

References

1- Fabian Kiessling and Bernd J Pichler, Small animal imaging: basics and practical guide. *Springer Science & Business Media*, (2010).

2- George C Kagadis, George Loudos, Konstantinos Katsanos, Steve G Langer, and George C Nikiforidis, "In vivo small animal imaging: current status and future prospects." *Medical physics*, Vol. 37 (No. 12), pp. 6421-42, (2010).

3- Min Wu and Jian Shu, "Multimodal molecular imaging: current status and future directions." *Contrast media & molecular imaging*, Vol. 2018(2018).

4- Robert S Miyaoka and Adrienne L Lehnert, "Small animal PET: a review of what we have done and where we are going." *Physics in Medicine & Biology*, Vol. 65 (No. 24), p. 24TR04, (2020).

5- Matthew A Kupinski and Harrison H Barrett, Small-animal SPECT imaging. *Springer*, (2005).

6- Steven R Meikle, Peter Kench, Michael Kassiou, and Richard B Banati, "Small animal SPECT and its place in the matrix of molecular imaging technologies." *Physics in Medicine & Biology*, Vol. 50 (No. 22), p. R45, (2005).

7- Annunziata D'Elia *et al.*, "Development of a high-resolution SSR-SPECT system for preclinical imaging and neuroimaging." *Nuclear Instruments and Methods in Physics Research Section A: Accelerators, Spectrometers, Detectors and Associated Equipment*, Vol. 1025p. 166161, (2022).

8- Yohji Matsusaka *et al.*, "Performance Evaluation of a Preclinical SPECT Scanner with a Collimator Designed for Medium-Sized Animals." *Molecular imaging*, Vol. 2022(2022).

9- Karen Van Audenhaege, Roel Van Holen, Stefaan Vandenberghe, Christian Vanhove, Scott D Metzler, and Stephen C Moore, "Review of SPECT collimator selection, optimization, and fabrication for clinical and preclinical imaging." *Medical physics*, Vol. 42 (No. 8), pp. 4796-813, (2015).

10- GR Gindi *et al.*, "Imaging with rotating slit apertures and rotating collimators." *Medical physics*, Vol. 9 (No. 3), pp. 324-39, (1982).

11- S Webb, MA Flower, and RJ Ott, "Geometric efficiency of a rotating slit-collimator for improved planar gamma-camera imaging." *Physics in Medicine & Biology*, Vol. 38 (No. 5), p. 627, (1993).

12- Roel Van Holen, Stefaan Vandenberghe, Steven Staelens, and Ignace Lemahieu, "Comparing planar image quality of rotating slat and parallel hole collimation: influence of system modeling." *Physics in Medicine & Biology*, Vol. 53 (No. 7), p. 1989, (2008).

13- Hojjat Mahani, Gholamreza Raisali, Alireza Kamali-Asl, and Mohammad Reza Ay, "Spinning slithole collimation for high-sensitivity small animal SPECT: Design and assessment using GATE simulation." *Physica Medica*, Vol. 40pp. 42-50, (2017).

14- D Uzun Ozsahin, Lisa Bläckberg, G El Fakhri, and H Sabet, "GATE simulation of a new design of pinhole SPECT system for small animal brain imaging." *Journal of Instrumentation*, Vol. 12 (No. 01), p. C01085, (2017).

15- MCM Rentmeester, F Van Der Have, and FJ Beekman, "Optimizing multi-pinhole SPECT geometries using an analytical model." *Physics in Medicine & Biology*, Vol. 52 (No. 9), p. 2567, (2007).

16- Lars R Furenlid *et al.*, "FastSPECT II: a second-generation high-resolution dynamic SPECT imager." *IEEE Transactions on Nuclear Science*, Vol. 51 (No. 3), pp. 631-35, (2004).

17- Freek J Beekman and Brendan Vastenhouw, "Design and simulation of a high-resolution stationary SPECT system for small animals." *Physics in Medicine & Biology*, Vol. 49 (No. 19), p. 4579, (2004).

18- Roberto Massari, Annunziata D'Elia, Andea Soluri, and Alessandro Soluri, "Super Spatial Resolution (SSR) method for small animal SPECT imaging: A Monte Carlo study." *Nuclear Instruments and Methods in Physics Research Section A: Accelerators, Spectrometers, Detectors and Associated Equipment*, Vol. 982p. 164584, (2020).

19- Johan Nuyts, Kathleen Vunckx, Michel Defrise, and Christian Vanhove, "Small animal imaging with multi-pinhole SPECT." *Methods*, Vol. 48 (No. 2), pp. 83-91, (2009).

20- Minh Phuong Nguyen, Marlies C Goorden, and Freek J Beekman, "EXIRAD-HE: multi-pinhole high-resolution ex vivo imaging of high-energy isotopes." *Physics in Medicine & Biology*, Vol. 65 (No. 22), p. 225029, (2020).

21- Gengsheng L Zeng and Daniel Gagnon, "CdZnTe strip detector SPECT imaging with a slit collimator." *Physics in Medicine & Biology*, Vol. 49 (No. 11), p. 2257, (2004).

22- Shelan T Mahmood, Kjell Erlandsson, Ian Cullum, and Brian Forbes Hutton, "Design of a novel slit-slat collimator system for SPECT imaging of the human brain." *Physics in Medicine & Biology*, Vol. 54 (No. 11), p. 3433, (2009).

23- Frans Van Der Have *et al.*, "U-SPECT-II: an ultra-high-resolution device for molecular small-animal imaging." *Journal of Nuclear Medicine*, Vol. 50 (No. 4), pp. 599-605, (2009).

24- Scott D Metzler, Roberto Accorsi, John R Novak, Ahmet S Ayan, and Ronald J Jaszczak, "On-axis sensitivity and resolution of a slit-slat collimator." *Journal of Nuclear Medicine*, Vol. 47 (No. 11), pp. 1884-90, (2006).

25- Etesam Malekzadeh, Hossein Rajabi, Elisa Fiorina, and Faraz Kalantari, "Derivation and validation of a sensitivity formula for knife-edge slit gamma camera: A theoretical and Monte Carlo simulation study." *Iranian Journal of Nuclear Medicine*, Vol. 29 (No. 2), pp. 86-92, (2021).

26- Roberto Accorsi, John R Novak, Ahmet S Ayan, and Scott D Metzler, "Derivation and validation of a sensitivity formula for slit-slat collimation." *IEEE transactions on medical imaging*, Vol. 27 (No. 5), pp. 709-22, (2008).

27- Martin J Berger and JH Hubbell, "XCOM: Photon cross sections on a personal computer." *National Bureau of Standards, Washington, DC (USA). Center for Radiation ...*, (1987).

28- P Cambraia Lopes *et al.*, "Optimization of collimator designs for real-time proton range verification by measuring prompt gamma rays." in *2012 IEEE Nuclear Science Symposium and Medical Imaging Conference Record (NSS/MIC)*, (2012): *IEEE*, pp. 3864-70.

29- Stephen C Moore, Kypros Kouris, and Ian Cullum, "Collimator design for single photon emission tomography." *European journal of nuclear medicine*, Vol. 19 (No. 2), pp. 138-50, (1992).